VARIATION OF PARAMETS METHOD FOR SQUEEZED FLOW OF A CASSON FLUID

by

Bandar BIN-MOHSIN*

Department of Mathematics, College of Science, King Saud University, Riyadh, Saudi Arabia

Original scientific paper
https://doi.org/10.2298/TSCI190708408B

The implementation of the variation of parameters method has been demonstrated for the flow of a Casson fluid through squeezed parallel plates. Governing PDE has been reduced, with the help of similarity transform, to relatively simpler ODE. The consequent non-linear equation is complicated enough to have an exact solution. We have solved that with the help of variation of parameters method. The results are displayed with the help of graphs and are decorated with suitable physical explanation.

Key words: *squeezing flow, Casson fluid, similarity transform, variation of parameters method.*

Introduction

Squeezing flows between parallel plates is of great importance and are widely used in polymer industry, hydromechanical models and many other industrial applications. Many researchers have made useful contributions in this field. In this context, the pioneering work has been delivered by Stefan [1] in 1874. Reynolds [2] demonstrated the squeezing flow of Newtonian fluid between parallel elliptic walls, this study can be further examined for rectangular channel by Archibald [3]. After this, numerous researchers have made a valuable contribution, some of them are highlighted in [4-8].

In literature, a variety of models have been found that captures the complex rheological features of most of the non-Newtonian fluids. The model for Cason fluid is among one of them, which is suitable for the non-Newtonian fluid-flows like blood flow [9, 10].

In this article, the squeezing flow of an unsteady Casson fluid (non-Newtonian fluid) have been considered between parallel plates. The transformed differential equations can be further tackled by employing variation of parameters method (VPM) [11-16]. The comparison results have shown an excellent agreement.

Mathematical model

An incompressible unsteady Casson fluid (non-Newtonian fluid) flow between squeezed parallel plates has been under consideration. Casson fluid has been elaborated by the following rheological equation:

* Author's e-mail: balmohsen@ksu.edu.sa

$$\tau_{pq} = \left[\mu_B + \left(\frac{p_y}{2\pi} \right)^{1/n} \right]^n 2e_{pq} \tag{1}$$

where e_{pq} is the $(p, q)th$ constituent of the rate of deformation rate. The yield stress for fluid is denoted by p_y while the plastic dynamic viscosity related to the non-Newtonian fluid is indicated by μ_B. The π signifies the product of component of deformation rate. Thus, the mathematical equations can be written:

$$\frac{\partial \breve{u}}{\partial \breve{x}} + \frac{\partial \breve{v}}{\partial \breve{y}} = 0 \tag{2}$$

$$\frac{1}{\rho}\frac{\partial \breve{p}}{\partial \breve{x}} + \frac{\partial \breve{u}}{\partial \breve{t}} + \left(\breve{v}\frac{\partial \breve{u}}{\partial \breve{y}} + \breve{u}\frac{\partial \breve{u}}{\partial \breve{x}} \right) = \upsilon \left(1 + \frac{1}{\beta} \right) \left(\frac{\partial^2 \breve{u}}{\partial \breve{y}^2} + 2\frac{\partial^2 \breve{u}}{\partial \breve{x}^2} + \frac{\partial^2 \breve{v}}{\partial \breve{y}\partial \breve{x}} \right) \tag{3}$$

$$\frac{1}{\rho}\frac{\partial \breve{p}}{\partial \breve{y}} + \frac{\partial \breve{v}}{\partial \breve{t}} + \left(\breve{v}\frac{\partial \breve{v}}{\partial \breve{y}} + \breve{u}\frac{\partial \breve{v}}{\partial \breve{x}} \right) = \upsilon \left(1 + \frac{1}{\beta} \right) \left(\frac{\partial^2 \breve{v}}{\partial \breve{y}^2} + 2\frac{\partial^2 \breve{v}}{\partial \breve{x}^2} + \frac{\partial^2 \breve{u}}{\partial \breve{y}\partial \breve{x}} \right) \tag{4}$$

where the kinematic viscosity is denoted by υ. The $\breve{p}$ is the pressure, while, $\beta = \mu_B \sqrt{2\pi_c} / p_y$ represents the Casson fluid parameter. Furthermore, the associated boundary conditions are defined:

$$\text{At } \breve{y} = h\left(\breve{t}\right), \quad \breve{u} = 0, \quad \breve{v} = v_w = \frac{\mathrm{d}h}{\mathrm{d}\breve{t}} \tag{5}$$

$$\text{At } \breve{y} = 0, \quad \frac{\partial \breve{u}}{\partial \breve{y}} = 0, \quad \breve{v} = 0 \tag{6}$$

By excluding the pressure term from eqs. (3) and (4) and by making use of eq. (2), the simplified system of equations have been achieved. Thus, introducing ω (the vorticity), we get the following equation:

$$\frac{\partial \omega}{\partial \breve{t}} + \breve{u}\frac{\partial \omega}{\partial \breve{x}} + \breve{v}\frac{\partial \omega}{\partial \breve{y}} = \upsilon \left(1 + \frac{1}{\beta} \right) \left(\frac{\partial^2 \omega}{\partial \breve{y}^2} + \frac{\partial^2 \omega}{\partial \breve{x}^2} \right) \tag{7}$$

where

$$\omega = \left(\frac{\partial \breve{v}}{\partial \breve{x}} - \frac{\partial \breve{u}}{\partial \breve{y}} \right) \tag{8}$$

Now the relevant similarity transforms has been introduced:

$$\breve{u} = \frac{\alpha \breve{x}}{2\left(1 - \alpha t\right)} A'\left(\eta\right), \quad \breve{v} = \frac{-\alpha l}{2\sqrt{1 - \alpha t}} A\left(\eta\right), \quad \eta = \frac{\breve{y}}{\sqrt{l\left(1 - \alpha t\right)}} \tag{9}$$

By making use of previous equation into the eq. (7) using (8), the subsequent non-linear ODE along with associated boundary condition for the flow of Casson fluid has been obtained:

$$\left(1 + \frac{1}{\beta} \right) A^{\mathrm{iv}}\left(\eta\right) - S\left\{ \left[\eta - A'''\left(\eta\right) \right] A\left(\eta\right) + \left[A'\left(\eta\right) + 3 \right] A''\left(\eta\right) \right\} = 0 \tag{10}$$

$$\text{For } \eta = 0, \; A\left(\eta\right) = 0, \; A''\left(\eta\right) = 0 \tag{11}$$

$$\text{For } \eta = 1,\ A(\eta) = 1,\ A'(\eta) = 0 \tag{12}$$

In previous equations, the dimensionless squeeze number is denoted by $S = \alpha l^2/2\upsilon$. The parting motion of the plates is signified by $S > 0$, while the squeezing motion is denoted by $S < 0$.

The coefficient for skin friction is elaborated:

$$C_f = v\left(1+\frac{1}{\beta}\right)\frac{1}{v_w^2}\left(\frac{\partial \tilde{u}}{\partial \tilde{y}}\right)_{\tilde{y}=h(\tilde{t})} \tag{13}$$

By making use of eq. (9), the dimensionless form for skin friction coefficient:

$$\frac{l^2}{x^2(1-at)}\mathrm{Re}_x C_f = \left(1+\frac{1}{\beta}\right)A''(1) \tag{14}$$

Variation of parameters method [11-16]

The following general ODE is considered to elucidate some basics about the VPM:

$$Lf(\xi) + Nf(\xi) + Xf(\xi) = g(\xi) \tag{15}$$

In the aforementioned equation, L, X, and N represent the highest order of linear operator, the linear operator of the order less than L, and the non-linear operator, respectively. Moreover, g is the source term and $f(\xi)$ is the solution of the differential equation. In the method under consideration, we can write the general approximate of the solution:

$$f(\xi) = \sum_{i=0}^{m-1}\frac{A_i}{i!}\xi^i - \int_0^{\xi}\lambda(\xi,\chi)\left[g(\chi) - Nu(\chi) - Xu(\chi)\right] \tag{16}$$

In eq. (7), m symbolizes the order of given differential equation. Furthermore, the unknown constants, $A_i s$, can be determined by using the auxiliary initial or boundary conditions. Furthermore, $\lambda(\xi, \chi)$ is the multiplier that reduces the order of integration and it can be determined by using the classical Wronskian technique. Some of the consequent expressions for the multiplier for different values of order are stated:

$$\begin{aligned} &m = 1,\ \ \lambda(\xi,\chi) = 1 \\ &m = 2,\ \ \lambda(\xi,\chi) = \xi - \chi \\ &m = 3,\ \ \lambda(\xi,\chi) = \frac{\xi^2}{2!} - \xi\chi + \frac{\chi^2}{2!} \\ &\vdots \end{aligned} \tag{17}$$

Equations (16) and (17) leads us to an iterative scheme that is given:

$$f_{k+1}(\xi) = \sum_{i=0}^{n-1}\frac{A_i}{i!}\xi^i - \int_0^{\xi}\lambda(\xi,\chi)\left[g(\chi) - Nf_k(\chi) - Xf_k(\chi)\right],\ \ k = 0,1,2,\ldots \tag{18}$$

At different levels of iterations, the previous iterative algorithm provides us the solution of the differential equation with sufficient auxiliary conditions. The terms outside the integral, provide us with an initial guess that initiates the iterative process. Its presence in all the iterations gives us a better approximation.

Solution procedure

An n^{th} order differential equation has been taken up to examine this technique:

$$a_n \frac{\mathrm{d}^n y(x)}{\mathrm{d}x^n} + a_{n-1} \frac{\mathrm{d}^{n-1} y(x)}{\mathrm{d}x^{n-1}} + \ldots + a_2 \frac{\mathrm{d}^2 y(x)}{\mathrm{d}x^2} + a_1 \frac{\mathrm{d}y(x)}{\mathrm{d}x} + a_0 y(x) = g(x) \tag{19}$$

with initial conditionism $y^m(0) = C_n$, $m = 0, 1, 2,..., n - 1$. Applying VPM, we get:

$$y_{n+1} = y_n + \int_0^x \lambda(s) \left[g(s) - a_{n-1} \frac{\mathrm{d}^{n-1} y}{\mathrm{d}s^{n-1}} + \ldots + a_1 \frac{\mathrm{d}y}{\mathrm{d}s} + a_0 y(s) \right] \mathrm{d}s, \quad y_0 = \sum_{m=0}^{n-1} \frac{C_m x^m}{m!} \tag{20}$$

where λ is a multiplier [12-14] and can be find optimally. Now, (12) can be re-written:

$$F_{j+1}(\eta) = F_j(\eta) + \int_0^\eta \lambda(s) \left\{ S \left[sF_j(s) + 3F_j''(s) + F_j'(s) F_j''(s) - F_j(s) F_j'''(s) \right] \right\} \mathrm{d}s \tag{21}$$

where $\lambda(s)$ is a multiplier [12-14].

Now, taking:

$$\lambda(s) = \frac{(x-s)^3}{3!} \ [12-14]$$

we get:

$$\begin{aligned} F(\eta) = {} & A\eta + \frac{1}{6} B\eta^3 + \frac{1}{40} \frac{S\beta B}{\beta+1} \eta^5 + \frac{1}{360} \frac{S\beta A}{\beta+1} \eta^6 + \\ & + \left[\frac{1}{560} \frac{S^2\beta^2 B}{(\beta+1)^2} - \frac{1}{840} \frac{S^2\beta^2 BA}{(\beta+1)^2} + \frac{1}{2520} \frac{S\beta B^2}{\beta+1} \right] \eta^7 + \\ & + \left[\frac{1}{6720} \frac{S^2\beta^2 A}{(\beta+1)^2} - \frac{1}{6720} \frac{S^2\beta^2 A^2}{(\beta+1)^2} + \frac{1}{10080} \frac{S\beta B}{\beta+1} \right] \eta^8 + \ldots \end{aligned} \tag{22}$$

Results and discussion

In this section, the behavior of radial, $A(\eta)$, as well as axial, $A'(\eta)$ velocities, under the action of varying values of squeeze number, S, and Casson fluid parameter, β, has been discussed. For this purpose, figs. 1-8 have been plotted. Figures 1 and 2 has been sketched to see the variation in radial, $A(\eta)$, as well as axial, $A'(\eta)$, velocities with varying values of squeeze number $S > 0$. It has been observed that the radial velocity decreases as S increases. On the other hand, as S increases, the axial velocity depicts a decreasing behavior in the lower half, for $\eta \leq 0.5$, however, an opposite behavior has been observed in the upper half, $0.5 < \eta \leq 1.0$.

The impact of Casson fluid parameter, β, on radial, $A(\eta)$, and axial, $A'(\eta)$, velocities, when squeeze number $S > 0$, have been presented in figs. 3 and 4, respectively. One can observe a decline in the radial velocity as β increases. Moreover, the axial velocity also depicts a declining behavior with growing β for $\eta \leq 0.5$, however, a reversed behavior for $A'(\eta)$ has been perceived in the upper half, $0.5 < \eta \leq 1.0$.

From fig. 5, one can see an increment in radial velocity, $A(\eta)$, as the squeeze number, S, decreases. Similarly, in the lower half, the axial velocity also depicts an increasing behavior with increasing S, however a decrement has been percieved in the upper half, *i. e.*, for $0.4 < \eta \leq 1.0$, see fig. 6.

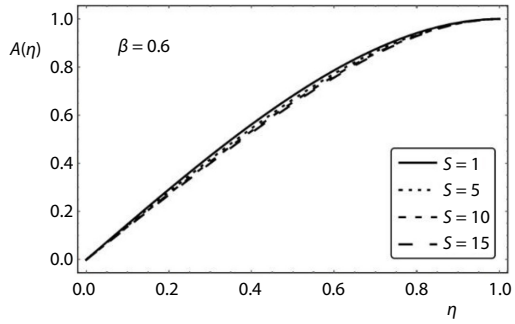

Figure 1. Behavior of $A(\eta)$, when $S > 0$

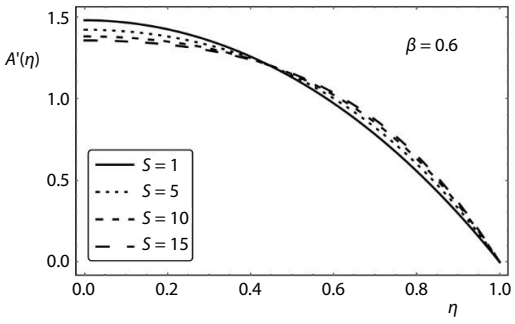

Figure 2. Behavior of $A'(\eta)$, when $S > 0$

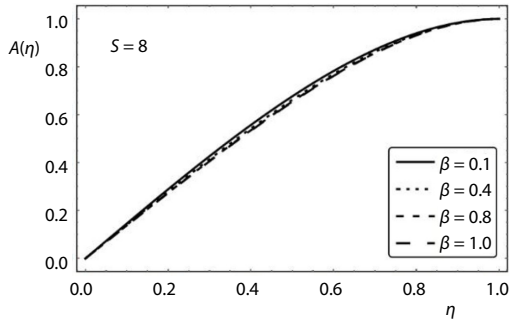

Figure 3. Behavior of $A(\eta)$, when $\beta > 0$ and $S > 0$

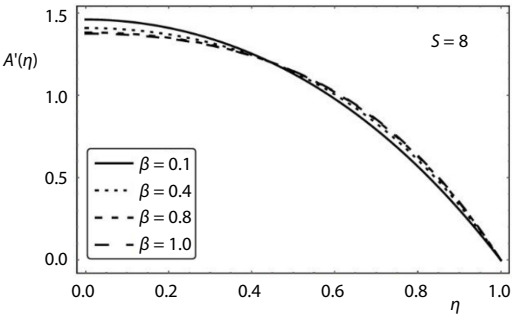

Figure 4. Behavior of $A'(\eta)$, when $\beta > 0$ and $S > 0$

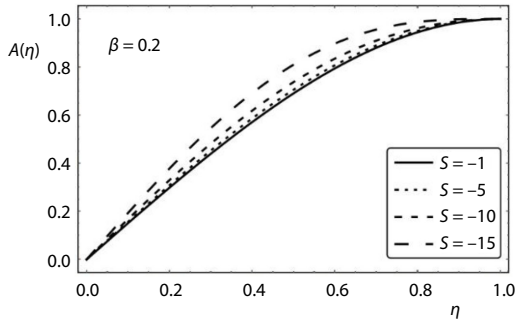

Figure 5. Behavior of $A(\eta)$, when $S < 0$

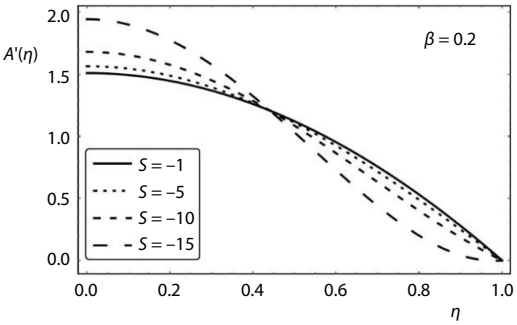

Figure 6. Behavior of $A'(\eta)$, when $S < 0$

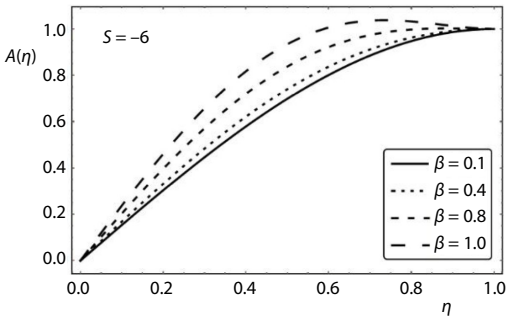

Figure 7. Behavior of $A(\eta)$, when $\beta > 0$ and $S < 0$

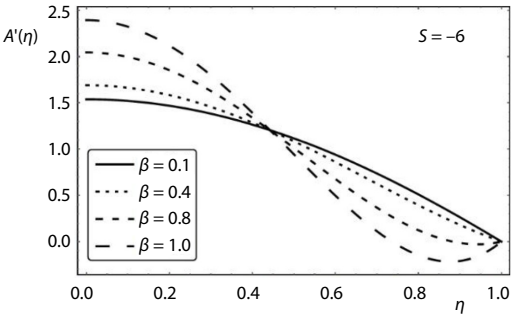

Figure 8. Behavior of $A'(\eta)$, when $\beta > 0$ and $S < 0$

Table 1. Numerical values for coefficient of skin friction

β	S	$\left(1+\frac{1}{\beta}\right)A''(1)$
0.4	0.5	–11.1265
–	1.5	–10.72315
–	–0.5	–10.26033
–	–1.5	–9.723203
0.5	–1.0	–8.25305
0.1	–	–32.2773
0.5	1.0	–9.68855
0.1	–	–33.7062

The case when squeeze number $S < 0$, the impact of varying values of β (Casson fluid parameter) on the radial, $A(\eta)$, and axial, $A'(\eta)$, velocities are depicted in figs. 5 and 6. Almost alike behavior has been observed for both $A(\eta)$ and $A'(\eta)$, as already been observed in figs. 3 and 4, respectively.

Table 1 provides the numerical results for coefficient of skin friction. It can be witnessed that magnitude of skin friction coefficient decreases as β increases. Moreover, by increasing S when $S > 0$, the magnitude of skin friction decreases, however an opposite behavior has been observed for $S < 0$.

The results for VPM and few previous studies are given in tabs. 2 and 3, for positive and negative values of squeeze number. The comparison presented here is showing that our results are very encouraging.

Table 2. Comparison of solutions, for $\beta = 0.8$, $S = 1$

η	*RK-F*	*VPM*	*DTM*	*LSM*
0.0	0	0	0	0
0.2	0.291426707190	0.291426707854	0.291426745210	0.291426707741
0.4	0.561062238797	0.561062231236	0.561062212358	0.561062238012
0.6	0.786049090612	0.786049090147	0.786049095863	0.786049090879
0.8	0.941540281235	0.941540284589	0.941540201423	0.941540281159
1.0	1	0.999999999998	0.999999999997	1.000000000001

Table 3. Comparison of solutions, for $\beta = 0.8$, $S = –1$

η	*RK-F*	*VPM*	*DTM*	*LSM*
0.0	0	0	0	0
0.2	0.301742965645	0.301742965852	0.301742961520	0.301742965641
0.4	0.576706786009	0.576706786123	0.576706781254	0.576706786036
0.6	0.799460459089	0.799460459754	0.799460459563	0.799460459095
0.8	0947079362361	0.947079362453	0.947079363657	0.947079362342
1.0	1	0.999999999999	0.999999999997	1.000000000001

Conclusion

In this study, the flow of a Casson fluid between squeezed parallel plates have been taken into account. Solutions of the transformed governing model has been found by using variation of parameters method. Comparison tabs. 2 and 3 reflect the credibility of the technique. Graphical aid have been provided to see the effect of various values (positive and negative) of squeeze number and Casson fluid parameter on axial as well as radial velocity components. The radial velocity decreaes as casson fluid parameter and positive squeezed number increases, however, the behavior is quite opposite for negative values of squeezed number.

Acknowledgment

Author thank the support of a grant from the Deanship of Scientific Research, King Saud University through Research Group RG-1437-019.

References

[1] Stefan, M. J., Versuch Uber die scheinbare adhesion, Sitzungsberichte der Akademie der Wissenschaften in Wien (in German), *Mathematik-Naturwissen*, *69* (1874), pp. 713-721
[2] Reynolds, O., On the Theory of Lubrication and Its Application mr. Beauchamp Tower's Experiments, Including an Experimental Determination of the Viscosity of Olive Oil, *Philosophical Transactions of the Royal Society of London*, *177* (1886), pp. 157-234
[3] Archibald, F., Load Capacity and Time Relations for Squeeze Films, *Journal of Lubrication Technology*, *78* (1956), pp. A231-A245
[4] Rashidi, M. M., *et al*., Analytic Approximate Solutions for Unsteady 2-D and Axisymmetric Squeezing Flows between Parallel Plates, *Mathematical Problems in Engineering*, *2008* (2008), ID 935095
[5] Siddiqui, A. M., *et al*., Unsteady Squeezing Flow of a Viscous MHD Fluid between Parallel Plates, A Solution Using the Homotopy Perturbation Method, *Mathematical Modelling and Analysis*, *13* (2008), 4, pp. 565-576
[6] Ahmed, N., *et al*., Effects on Magnetic Field in Squeezing Flow of a Casson Fluid between Parallel Plates, *Journal of King Saud University – Science*, *47* (2015), 7, pp. 1581-1589
[7] Saba, F., *et al*., A Novel Coupling of (CNT-Fe_3O_4/H_2O) Hybrid Nanofluid for Improvements in Heat Transfer for Flow in an Asymmetric Channel with Dilating Squeezing Walls, *International Journal of Heat and Mass Transfer*, *136* (2019), June, pp. 186-195
[8] Saba, F., *et al*., Impact of an Effective Prandtl Number Model and Across Mass Transport Phenomenon on the γAI_2O_3 Nanofluid-Flow inside a Channel, Physica A: *Statistical Mechanics and its Applications*, *526*, (2019), Apr., 121083
[9] Mrill, E. W., *et al*., Pressure Flow Relations of Human Blood Hollow Fibers at Low Flow Rates, *Journal Appl. Physiol*., *20* (1965), 5, pp. 954-967
[10] McDonald, D. A., *Blood Flows in Arteries*, 2nd ed., Arnold, London, 1974
[11] Mohyud-Din, S. T. *et al*., Magnetohydrodynamic Flow and Heat Transfer of Nanofluids in Stretchable Convergent/Divergent Channels, *Applied Sciences*, *(MDPI)*, *5* (2015), 4, pp. 1639-1664
[12] Mohyud-Din, S. T. *et al*., Thermo-Diffusion, Diffusion-Thermo and Chemical Reaction Effects on Flow of Micropolar Fluid of Asymmetric Channel with Dilating and Contracting Permeable Walls, *Engineering Computations, (Emerald)*, *34* (2017), 2, pp. 587-602
[13] Ramos, J. I., On the Variational Iteration Method and Other Iterative Techniques for Non-Linear Differential Equations, *Applied Mathematics and Computation*, *199* (2008), 1, pp. 39-69
[14] Khan, U., *et al*., Influence of the Shape Factor on the Flow and Heat Transfer of a Water-Based Nanofluid in a Rotating System, *European Physical Journal Plus*, *132* (2017), 4, p. 166
[15] Sikander, W., *et al*., Optimal Solutions for Homogeneous and Non-Homogeneous Equations Arising in Physics, *Results in Physics*, *7* (2017), Dec., pp. 216-224
[16] Sikander, W., *et al*., Coupling of Optimal Variation of Parameters Method with Adomian's Polynomials for Non-Linear Equations Representing Fluid-Flow in Different Geometries, *Neural Computing and Applications*, *30* (2018), 11, pp. 3431-3444

Paper Submitted: July 8, 2019
Paper revised: October 13, 2019
Paper accepted: October 15, 2019